Transport of Long-Chain Native Fatty Acids across Lipid Bilayer Membranes Indicates That Transbilayer Flip-Flop Is Rate Limiting†

Alan M. Kleinfeld,* Peter Chu, and Carol Romero

Medical Biology Institute, 11077 North Torrey Pines Rd., La Jolla, California 92037

Received June 16, 1997; Revised Manuscript Received August 28, 1997⊗

ABSTRACT: Evidence from a number of laboratories suggests that membrane proteins may meditate the transport of physiologic fatty acids (FA) across cell membranes. However, studies using lipid membranes indicate that FA are capable of spontaneous flip-flip, raising the possibility that rapid transport through the lipid phase obviates the need for a transport protein. Determining the rate-limiting steps for transport of FA across lipid membranes, therefore, is central to understanding FA transport across cell membranes. The transport of long-chain FA across lipid membranes, from the aqueous compartment on one side of the lipid bilayer to the aqueous phase on the other side, has not been measured previously. In this study, we have used the fluorescent probe ADIFAB to monitor the time course of FA movement from the outer to the inner aqueous compartments and from the lipid membrane to the outer aqueous compartment of lipid vesicles. These two measurements, together with measurements of the lipid:aqueous partition coefficients, allowed the determination of the rate constants for binding (k_{on}), flip-flop (k_{ff}), and dissociation (k_{off}) for the transport of long-chain natural FA across lipid vesicles. These rates were determined using large unilamellar vesicles (LUV) of approximately 1000 Å diameter, prepared by extrusion and giant unilamellar vesicles (GUV), prepared by detergent dialysis, that are ≥2000 Å diameter. The results of these studies for vesicles composed of egg phosphatidylcholine (EPC) and cholesterol reveal k_{ff} values that range from 3 to 15 s^{-1} for LUV and from 0.1 to 1.0 s^{-1} for GUV, depending upon temperature and FA type. For these same vesicles, dissociation rate constants range from 4 to 40 s^{-1} for LUV and from 0.3 to 2.5 s^{-1} for GUV. In all instances, the rate constant for flip-flop is smaller than k_{off}, and because the rate of binding is greater than the rate of transport, we conclude that flip-flop is the rate-limiting step for transport. These results demonstrate that (1) k_{ff} and k_{off} are smaller for GUV than for LUV, (2) the rate constants increase with FA type according to oleate (18:1) < palmitate (16:0) < linoleate (18:2), and (3) the barrier for flip-flop has a significant enthalpic component. Comparison of the flip-flop rates determined for GUV with values estimated from previously reported metabolic rates for cardiac myocytes, raises the possibility that flip-flop across the lipid phase alone may not be able to support metabolic requirements.

Elucidating the mechanism by which fatty acids (FA)[1] are transported across cell membranes is important for understanding FA metabolism. Although this issue has received considerable study, disagreement remains over the question of whether metabolic requirements can be satisfied by spontaneous transport of FA through the lipid phase of the membrane or whether intervention by a membrane transport protein is required [reviewed in Kleinfeld (1995)]. In principal, it should be possible to resolve this issue by determining if FA transport through lipid bilayers is rapid enough so that protein mediation would be unnecessary for cellular transport. Considerable effort, therefore, has been devoted to determining the rates and mechanism of transbilayer transport of FA across lipid bilayers, but the conclusions of these different studies are contradictory (Doody et al., 1980; Walter & Gutknecht, 1984; Storch & Kleinfeld, 1986; Kleinfeld & Storch, 1993; Kamp et al., 1995; Kleinfeld, 1995).

Transport across membranes can be viewed as three separate steps. First, FA move from the aqueous phase to the membrane surface (on-step). Second, FA move from one hemileaflet of the bilayer to the other hemileaflet (flip-flop). Third, FA move from the bilayer into the aqueous phase (off-step). Although any one of these steps might be rate limiting, by most estimates the on-step is fast and therefore not rate limiting (see Results and Table 3). Thus, the controversy associated with the nature of the lipid bilayer as a barrier to long-chain FA transport is whether the off-step or flip-flop is rate limiting and for either rate-limiting step whether it is limiting for metabolic activity.

Because long-chain FA are poorly soluble, previous investigations of this issue have not measured the actual transport of long-chain FA between the aqueous compartments on either side of the bilayer, except for the preliminary studies discussed in (Kleinfeld, 1995). In most previous studies, flip-flop and off rates were inferred from measurements of transfer between lipid vesicles or between vesicles and acceptor proteins. Results from these earlier studies are consistent with either the off-step (Doody et al., 1980;

† This work was supported by grant GM44171 from the NIH.

* To whom correspondence should be addressed.

⊗ Abstract published in *Advance ACS Abstracts,* November 1, 1997.

[1] Abbreviations: 2-AOSA, 2-AO-stearic acid; ADIFAB, rat intestinal fatty acid binding protein labeled at Lys^{27} with acylodan; AOFA, anthroyloxy fatty acid; CF, carboxyfluorescein; EPC, egg phosphatidylcholine; FA, fatty acid; FFA, free fatty acid; GUV, giant unilamellar vesicles; LUV, large unilamellar vesicles; NBD-PE, *N*-(7-nitro-2,1-phosphatidylethanolamine; SUV, small unilamellar vesicles.

S0006-2960(97)01440-2 CCC: $14.00

Daniels et al., 1985) or flip-flop (Storch & Kleinfeld, 1986; Kleinfeld & Storch, 1993) as rate limiting. More recently, studies have been done to detect the movement of both native (unlabeled) and the anthroyloxy-labeled FA (AOFA) from the outer to the inner hemileaflet of the bilayer after adding FA to the outer aqueous phase of lipid vesicles (Kamp et al., 1995). In these measurements, FA flip-flop was monitored by detecting, with the pH sensitive fluorophore pyranine trapped within the lipid vesicle, the release of H^+ as protonated FA moved from the outer to the inner hemileaflet of the bilayer. This configuration provides a more direct measurement of flip-flop than those in which transfer is measured between vesicles or vesicles and proteins. The results of these studies yielded flip-flop rates that were extremely rapid (<30 ms), and within a factor of 2, these rates were independent of FA chain length and the attachment of the anthroyloxy group.

We have recently reinvestigated flip-flop of the AOFA across lipid vesicles using the pyranine methodology developed by Kamp et al. (1995) and a new method, in which carboxyfluorescein trapped within lipid vesicles serves as a resonance energy transfer acceptor to detect movement of the AOFA from outer to inner bilayer leaflet (Kleinfeld et al., 1997b). In contrast to the results of Kamp et al. (1995), these new results indicate that flip-flop of long (16 carbon)-chain AOFA requires more than 50 s and is rate limiting. Moreover, measurements done with the shorter chain (11 carbon) AOFA reveal flip-flop rates that are more than 50-fold faster than for the long-chain AOFA, indicating that the rate of flip-flop is highly sensitive to the structure of the FA. The results of these new measurements are in excellent agreement with our earlier results obtained from measurements of intervesicle transfer (Storch & Kleinfeld, 1986; Kleinfeld & Storch, 1993). These earlier results showed that the rates of flip-flop of the long-chain anthroyloxy FA (AOFA) across lipid vesicles were slower than the rate at which these FA either dissociate from or bind to the bilayer surfaces of these vesicles and, therefore, that flip-flop is rate limiting for lipid bilayer transport of the long-chain AOFA.

Although transport of the long-chain AOFA across lipid bilayers is slow and rate limiting, it is not clear that the long-chain native FA possess the same characteristics. Transport of long-chain FA between aqueous phases have not been measured previously, principally because the aqueous phase concentration of the long-chain FA could not be measured accurately. This limitation can be overcome using ADIFAB, the fluorescent probe of free fatty acids (FFA) (Richieri et al., 1992). In preliminary studies, we have demonstrated that this probe has sufficient sensitivity and temporal resolution to monitor FFA transport across membranes, and these preliminary results reveal times of several seconds for transport of long-chain native FA across lipid vesicles (Kleinfeld, 1995). In the present report, we describe this methodology in detail and apply this approach to the determination of all three rate constants (k_{on}, k_{ff}, and k_{off}) that define transbilayer transport of FFA in a variety of lipid vesicles. Using ADIFAB trapped within lipid vesicles, we have confirmed the transport rates observed in our preliminary studies, and we have demonstrated that flip-flop is the rate-limiting step for transport of long-chain native FA across large unilamellar vesicles. The flip-flop rates determined by ADIFAB in GUV were also confirmed using the pyranine method of Kamp et al. (1995).

MATERIALS AND METHODS

Materials. Egg phosphatidylcholine (EPC) and *N*-(7-nitro-2,1-phosphatidylethanolamine (NBD-PE) was purchased from Avanti Polar-Lipids, Inc. (Alabaster, AL), and cholesterol was from (Nu Chek Prep, Elysian MN). [^{3}H]DPPC (phosphatidylcholine, L-α-dipalmitoyl, [choline-methyl-^{3}H]) was from American Radiolabeled Chemicals, Inc. (St. Louis, MO). Pyranine (8-hydroxyprene-1,3,6-trisulfonic acid) and 2-anthroyloxy stearate (2-AOSA) was purchased from Molecular Probes (Eugene, OR). ADIFAB was prepared as described (Richieri et al., 1992) and is available from Molecular Probes (Eugene, OR). For all measurements, the sodium salts of the FA (Nu Chek Prep, Elysian, MN) were used, as described previously (Richieri et al., 1992, 1994, 1995). Stock solutions of the FA salt were prepared in 20 mM KOH and were maintained under argon at −20 °C. The buffer used to measure FA transport, dissociation, and binding using ADIFAB consisted of 20 mM HEPES, 150 mM NaCl, 5 mM KCl, and 1 mM $NaHPO_4$, at pH 7.4. The buffer for the pyranine-containing vesicles was 100 mM HEPES and 50 mM NaCl at pH 7.5.

Vesicle Preparation. Two types of vesicles were used in this study. The first were unilamellar vesicles of approximately 1000 Å diameter prepared by the extrusion method, essentially as described (Hope et al., 1985; Anel et al., 1993), and are designated large unilamellar vesicles (LUV). EPC or EPC plus cholesterol was dissolved in chloroform and evaporated to dryness in a rotary evaporator. For mixtures of EPC and cholesterol, the dried lipid film was redissolved in *tert*-butanol and evaporated to dryness. For all compositions, the dried film was protected from air, following evaporation, by allowing argon to fill the flask containing the dried lipid film, after releasing the vacuum in the rotary evaporator. The dried film was lyopholized overnight, covered with argon, and then hydrated in buffer. For vesicles containing trapped ADIFAB or pyranine, 400 μM ADIFAB or 500 μM pyranine was included in the buffer. Hydrated vesicles were subjected to five cycles of freezing and thawing and were then passed 11 times through two 0.1 μm polycarbonate filters (Nuclepore) at room temperature using a Lipex Extruder (Lipex Biomembranes, Vancouver, B.C). For ADIFAB-containing vesicles, the hydrated suspension was prefiltered through 1.0 μm and 0.2 μm polycarbonate filters before passage 11 times through the stacked 0.1 μm filters. Vesicles containing trapped fluorophore were separated from free fluorophore using Sephacryl-1000 chromatography.

The second type of vesicles, designated here as giant unilamellar (GUV) vesicles, were prepared by octyl-β-glucopyranside (OG) solubilization/dialysis, and these vesicles are ≥2000 Å in diameter (Nozaki et al., 1982; Kleinfeld & Storch, 1993; Marassi et al., 1993; Franzin & Macdonald, 1997). Lipid preparation and hydration were similar to that for LUV, except that the hydrated suspension was not subjected to freeze−thawing. Lipid suspensions in the dialysis membranes were 0.5−1 mL and were dialyzed at 4 °C against four changes of buffer of 4 L each, over 4 days. Following dialysis, the suspension was centrifuged at 1500*g* for 5 min to remove very large vesicles (>1 μm) that were found to impede Sephacryl-1000 chromatography. Examination of these large vesicles by fluorescence microscopy indicated that they did not seal. The remaining vesicles were

chromatographed on Sephacryl-1000 to remove free ADIFAB.

Sephacryl-1000 elution profiles for both LUV and GUV were determined by monitoring the trace [^{3}H]DPPC included in all preparations and fluorescence, in those preparations in which fluorophore was trapped. For each preparation, the phospholipid and cholesterol concentrations were determined for (1) the unfractionated vesicles (after extrusion or dialysis but before centrifugation or chromatography), (2) the very large vesicles that pelleted at 1500*g*, and (3) the vesicles that eluted from the Sephacryl-1000 column. Phospholipid concentration was determined as inorganic phosphate (Gomori, 1942), and cholesterol was determined using a cholesterol oxidase assay (Sigma, St. Louis, MO). In general, the EPC/cholesterol ratios of the unfractionated vesicles and LUV were similar while for the GUV, this ratio was larger for the GUV than the unfractionated vesicles but was smaller for the large pelleted vesicles. Vesicle concentration in all measurements was between 50 and 100 μM EPC. Representative vesicle preparations were analyzed by thin layer chromatography as described previously (Kleinfeld & Storch, 1993) and showed no evidence of significant lipid degradation.

Fluorescence Instrumentation. Steady state fluorescence measurements were done using either an SLM 4800 or an SLM 8100 fluorometer (Kleinfeld et al., 1997b). AOFA fluorescence was measured using excitation and emission wavelengths of 383 and 450 nm, respectively, pyranine fluorescence was monitored at 455 and 509 nm, respectively, NBD-PE was monitored at 450 nm excitation and 550 nm emission, and ADIFAB was monitored at 386 nm excitation and emission wavelengths of 505 and 432 nm. Initial stopped-flow measurements were done using an SLM Milliflow device coupled to the SLM8100 fluorometer. Most of the stopped-flow fluorescence was measured using a KinTek Instrument (State College, PA) in which equal volumes (about 0.1 mL) of reactants were mixed with a dead time of <2 ms as described previously (Richieri et al., 1996b). Fluorescence was measured using two photomultipliers placed on opposite sides of the viewing chamber, and intensities were monitored through 20 nm band width filters centered at 432 and 505 nm (Omega optical, Brattleboro, VT). A minimum of five scans was acquired for each condition, and approximately 500 data points were collected per scan, and both instruments gave equivalent results.

Determination of Vesicle Lamellarity. Previous studies are consistent with the predominantly unilamellar character of vesicles prepared by extrusion or detergent dialysis (Nozaki et al., 1982; Hope et al., 1985; Marassi et al., 1993; Comfurius et al., 1996; Franzin & Macdonald, 1997). Nevertheless, because transport might be slowed through multilamellar vesicles, we have assayed the lamellarity of vesicles used in these studies. These assays used the membrane impermeant fluorescence quenchers, cobalt (Cardoza et al., 1984; Homan & Eisenberg, 1985; Morris et al., 1985) and dithionite (McIntyre & Sleight, 1991), to determine the accessibility of the membrane-bound fluorophores, 2-AOSA and NBD-PE, respectively. These fluorophores, at levels of 0.1% NBD-PE and 2% 2-AOSA, respectively, were included in the preparation of LUV composed of EPC and EPC:cholesterol 2:1 and GUV composed of EPC and EPC:cholesterol 2:1 and 3:1. In selected cases, ADIFAB was also included in the preparation with NBD-PE or 2-AOSA and transport properties for these vesicles were found to be virtually indistinguishable from vesicles without the membrane bound fluorophores (data not shown). Measurements of cobalt quenching of 2-AOSA fluorescence were done by titrating vesicles dispersed in 3×3 mm path length cuvettes with 0−50 mM $CoCl_2$, and the observed intensities were corrected for cobalt absorbance (inner filter correction). Quenching of NBD-PE was done by adding between 7 and 15 mM sodium dithionite to the vesicle suspension. For both types of vesicles, measurements were done at room temperature, and the maximum degree of quenching was determined by subjecting the vesicles to five cycles of freezing and thawing in the presence of the maximum concentration of quencher.

Table 1: Vesicle Lamellarity Determined by Fluorescence Quenching[a]

	LUV[b]	GUV[c]
2-AOSA	49	42
NBD-PE	45	39

[a] Values are I/I_o in percent, where I_o is the initial fluorescence intensity of either 2-AOSA or NBD-PE incorporated in the lipid vesicles, and I is the intensity when the concentration of the cobalt or dithionite quencher is maximum. The I/I_o value is corrected for dilution and inner filter effects for cobalt. [b] LUV, averages of four and three independent measurements for 2-AOSA and NBD-PE, respectively, for vesicles composed of EPC and EPC:cholesterol 2:1. Standard deviations were about 10% I/I_o. [c] GUV, average of four and five independent measurements for 2-AOSA and NBD-PE, respectively, for vesicles composed of EPC:cholesterol 2:1 and 3:1. Standard deviations were about 10% I/I_o.

For all vesicles, we observed that, between 39 and 49% of the 2-AOSA and NBD-PE, fluorescence intensities were quenched by cobalt and dithionite, respectively (Table 1). These values of quenching reflect a minimum amount of the fluorophore that is accessible because electrostatic repulsion by Co^{2+} absorbed to neutral lipid membrane prevents complete quenching (Homan & Eisenberg, 1985), and variable amounts (10−40%) of residual fluorescence were observed in NBD-PE-containing vesicles that were subjected to freeze−thaw in the presence of dithionite. Moreover, the maximum degree of quenching expected for EPC LUV is 59% because of the asymmetry of the outer to inner areas of these vesicles, but our quenching measurements reveal an average of 47% for quenching of these vesicles, further supporting the presence of residual fluorescence even under conditions that should yield complete quenching. Thus, the values shown in Table 1 represent minimum values for the ratio ($r_{o/i}$) of outer hemileaflet to inner lamelli areas. These values can be used to calculate the average number of lamelli per vesicle (n), using $n = (1 + r_{o/i})/(2r_{o/i})$, (Meyuhas & Lichtenberg, 1996), from which we obtain average values of 1.06 and 1.23, for LUV and GUV, respectively. Recognizing that these are maximum values for n because the $r_{o/i}$ used in this calculation are the minimum values shown in Table 1, we conclude that the vesicles are predominantly unilamellar. Indeed, if we assume that the LUV are unilamellar (consistent with previous determinations (Hope et al., 1985), the 47% quenching observed for LUV implies that quenching values should be increased by 1.25 to achieve the expected 59% level, and this factor would yield a value of n for GUV equal to 1.0.

Vesicle Integrity. Vesicle integrity to ADIFAB and/or pyranine leakage was assessed using fluorescence quenching.

Sodium molybdate (Na_2MoO_4) quenches ADIFAB fluorescence (at 432 nm) by what appears to be a collision-mediated mechanism, yielding for 50 mM Na_2MoO_4 about 40% quenching of free ADIFAB and less than about 3% when ADIFAB is trapped in vesicles (data not shown). Similarly, free pyranine is quenched by about 80% by 20 mM $CoCl_2$ and less than 1% when trapped in vesicles (data not shown).

Partition Coefficients. Coefficients of FA partition (K_p) between buffer and lipid vesicles were determined as described previously (Anel et al., 1993; Richieri et al., 1995). Briefly, FA were added to a solution containing 0.5 μM ADIFAB plus between 50 and 100 μM (phospholipid) lipid vesicles, and this mixture was allowed to incubate for 10 min at 20, 30, and 37 °C. After the incubation period, the ratio of the ADIFAB fluorescence emission intensities at 505 to 432 nm (R value) was measured and [FFA] was determined as previously described (Richieri et al., 1992). The partition coefficient was computed as $K_p = [([FA_T] - [FFA])/[FFA]]V_a/V_m$, where $[FA_T]$ is the total FA concentration in the cuvette, and V_a and V_m are the volumes of aqueous and membrane phases, respectively, and a value of 10^{-6}/M phospholipid was used for V_m/V_a (Anel et al., 1993). Measurements were done for LUV and GUV composed of EPC and EPC:cholesterol, and virtually identical results were obtained with both types of vesicles and all compositions and temperatures. Averages for all measurements were consistent with our previous results (Anel et al., 1993; Richieri et al., 1995) and yielded 5×10^5, 4×10^5, and 1.5×10^5 for palmitate, oleate, and linoleate, respectively.

Determination of Rate Constants for FA Dissociating From, Transferring Across, and Binding to Lipid Vesicles. To determine the rate constants (k_{off}, k_{ff}, and k_{on}) that characterize FA transport across membranes, time courses of FA movement, corresponding to different arrangements of FA, vesicles, and ADIFAB, were analyzed using the following sets of equations that describe each of the types of measurements:

$$\frac{d[ADIFAB_b]}{dt} = -k_{off}^{AF}[ADIFAB_b] + k_{on}^{AF}[ADIFAB_f][FFA_{i,o}] \quad (1)$$

$$\frac{d[FFA_o]}{dt} = k_{off}^{AF}[ADIFAB_b] + k_{off}[FAm_o] - (k_{on}^{AF}[ADIFAB_f] + k_{on}[L])[FFA_o] \quad (2a)$$

$$\frac{d[FFA_o]}{dt} = +k_{off}[FAm_o] - k_{on}[L][FFA_o] \quad (2b)$$

$$\frac{d[FAm_o]}{dt} = -k_{off}[FAm_o] + k_{on}[L][FFA_o] + k_{ff}([FAm_i] - [FAm_o]) \quad (3)$$

$$\frac{d[FAm_i]}{dt} = k_{ff}([FAm_o] - [FAm_i]) \quad (4)$$

$$\frac{d[FFA_i]}{dt} = k_{off}[FAm_i] - k_{on}[L][FFA_i] \quad (5a)$$

$$\frac{d[FFA_i]}{dt} = k_{off}^{AF}[ADIFAB_b] + k_{off}[FAm_i] - (k_{on}^{AF}[ADIFAB_f] + k_{on}[L])[FFA_i] \quad (5b)$$

FA binding and dissociation rate constants for ADIFAB are denoted k_{on}^{AF} and k_{off}^{AF}, respectively, k_{on}, k_{off}, and k_{ff} are the respective rate constants for the bilayer, the subscripts b and f designate bound and free (total-bound) ADIFAB concentrations, respectively, $[FAm_{o,i}]$ is the concentrations of FA in the outer and inner leaflet of the bilayer, respectively, $[FFA_{o,i}]$ is the FFA concentration in the outer and inner aqueous phase, respectively, and [L] is the vesicle lipid concentration.

Stopped-flow measurements were done in which, (1) FA were equilibrated with vesicles in one syringe and then mixed with ADIFAB in a second syringe, primarily to determine k_{off}, and (2) vesicles containing trapped ADIFAB or pyranine were mixed with FA to determine k_{ff}. With appropriate boundary conditions, eqs 1−5 describe the models used to analyze the time courses resulting from these measurements. The following equations and initial conditions ($t = 0$) apply to each of these types of measurements. For analysis of FA dissociation from the vesicles, eqs 1, 2a, 3, 4, and 5a were used with the subscript o applying to eq 1. The initial ($t = 0$) conditions for this analysis are $[ADIFAB_b] = 0$, and the initial values for $[FAm_o]$, $[FAm_i]$, and $[FFA_o]$ were determined from the equilibrium condition that exists before mixing. Thus, $[FAm_o] = [FAm_i] = FA_T/2(1 + 1/K_p[L])$, and $[FFA_o] = FA_T - 2[FAm]$, where FA_T is the total concentration of FA in the reaction mixture, [L] is the lipid concentration of the vesicles, and K_p is the partition coefficient. For the transport measurements, eqs 1, 2b, 3, 4, and 5b apply with the subscript i used in eq 1. The initial conditions for this case are $[ADIFAB(0)]_b = [FAm_i] = [FAm_o] = [FFA_i] = 0$ and $[FFA_o] = FA_T$. In addition to determining k_{off} and k_{ff} from these kinetic measurements, k_{on} values were calculated as $k_{on} = K_p k_{off}$ and $K_p k_{off}$ was substituted for k_{on} in eqs (2, 3, and 5).[2]

The quantity that is actually measured in these studies is the time-dependent change in the ratio $[R(t)]$ of the fluorescence intensity of ADIFAB at 505 and 432 nm. As described previously (Richieri et al., 1996a), $R(t)$ can be expressed in terms of solutions to eqs 1−5:

$$R(t) = \frac{R_o + 0.59X(t)}{1 + 0.05X(t)} \quad (6)$$

where R_o is the value of R in the absence of FA, and the numerical constants were obtained from the spectral properties of ADIFAB as described previously (Richieri et al., 1992), and

[2] The relationship $k_{on} = K_p k_{off}$ follows, at low FA to membrane lipid ratios, from the definition of the partition coefficient. Thus, we take $K_p = V_a[FA_m]/V_m[FFA]$ where $[FA_m] = [FA_T] - [FFA]$ (Anel et al., 1993 and Materials and Methods) and for the association constant for FA binding (K_a) to the membrane, $K_a = [FA_m]/([FFA][L_f])$, where $[L_f]$ is the concentration of membrane lipid not complexed with FA (free). For low FA to membrane lipid ratios, $[L_T] \approx [L_f]$ and it follows that $K_a \approx K_p V_m/[L_T]V_a$. Using $V_m/V_a \approx [L_T]$, we get $K_a = k_{on}/k_{off} \approx K_p$.

$$X(t) = \frac{[\mathrm{ADIFAB}(t)]_b}{[\mathrm{ADIFAB}]_T - [\mathrm{ADIFAB}(t)]_b} \quad (7)$$

where $[\mathrm{ADIFAB}]_T$ is the total concentration of ADIFAB in the final mixture.

To obtain the rate constants, it is necessary to fit the measured $R(t)$ values with the values predicted by eq 6. This can be done using the program MLAB (Civilized Software, Bethesda, MD) which determines the model parameters by using a Marquardt−Levenberg minimization to fit numerical solutions of eqs 1−5 and measured $R(t)$ values, as described previously (Richieri et al., 1996a,b; Kleinfeld et al., 1997b). The quality of fit was assessed by the sum of squares of the theory-experiment differences (SOSQ), fit residuals, and direct observation and generally gave excellent agreement between theory and experiment.

Only numeric solutions for the transport time course are available for the full set of eqs 1−5. However, because the amount of FA that binds to ADIFAB trapped within the vesicles is generally less than 10% of FA_T and because the rates of binding and dissociation for ADIFAB (Richieri et al., 1996a) are considerably faster than the rate at which FA is transported across the vesicles, the ADIFAB dependence in eqs 1−5 can be eliminated and the remaining four equations can be solved analytically as described in Kleinfeld (1995). This analytic solution for $[FFA_i(t)]$ is

$$[FFA_i(t)] = e^{-\beta t}\left(\frac{(c_0\beta - c_0 - 2c_0k_{ff})\sinh\left(t\frac{\gamma}{2}\right)}{\gamma} - \frac{c_0\cosh\left(t\frac{\gamma}{2}\right)}{2}\right) + \frac{c_0(k_{on}l e^{-(k_{on}l + k_{off})t} + k_{off})}{2(k_{on}l + k_{off})} \quad (8)$$

in which

$$\beta = \frac{(k_{on}l + k_{off} + 2k_{ff})}{2}$$

and

$$\gamma = \sqrt{k_{on}^2l^2 + (2k_{off} - 4k_{ff})k_{on}l + k_{off}^2 + 4k_{ff}k_{off} + 4k_{ff}^2}$$

where l is the vesicle lipid concentration and c_0 is the initial FA concentration (FFA_T).

$R(t)$ can be calculated from $[FFA_i(t)]$ (eq 8) using the equation relating [FFA] and R (Richieri et al., 1992). Fitting this expression to the time course for transport, using MLAB, yields virtually identical rate constants as the numeric solution of the full set of eqs 1−5. The analytic expression provides a clearer understanding of how the time courses depend on the rate constants and can be used with conventional fitting algorithms (Bevington & Robinson, 1992).

Simulated Time Courses of Dissociation from, Transport across, and Binding to Lipid Vesicles. In this study, off-rate constants, k_{off}, were determined by measuring the time course of FA dissociation from vesicles, using the change in ADIFAB fluorescence to monitor FA as it moves from the outer hemileaflet of the vesicle and binds to ADIFAB in the extravesicular medium. These measurements were done by stopped-flow mixing of FA−vesicle complexes in one syringe with increasing concentrations of ADIFAB in the second syringe. Time courses expected for such measurements were simulated using the solutions of eqs 1−5 to predict how $R(t)$ depends upon the vesicle rate constants (Figure 1A). These results show that $R(t)$ increases monotonically from R_o when no FFA is present in the medium, to an equilibrium value that is approached asymptotically. The rate of change of $R(t)$ is fastest at ADIFAB concentrations ≤1 mM, because at these low concentrations, the time course reflects the fraction of FA that is initially free in equilibrium with the vesicles and therefore is dependent only on the ADIFAB rate constants (not shown). As the ADIFAB concentration increases (≥2 μM), a significant fraction of the FA initially bound to the vesicles redistributes to ADIFAB and the time course now also reflects the vesicle rate constants. In separate measurements, we determined that FA partitioned equally between vesicle and ADIFAB at lipid and ADIFAB concentrations of about 50 and 20 μM, respectively (data not shown). If $k_{ff} < k_{off}$, then most of the FA transferred to ADIFAB at moderate concentrations (<10 μM) will reflect dissociation of FA from the outer hemileaflet into the extravesicular aqueous medium. Consequently, the time courses for these ADIFAB concentrations provide a sensitive measure of k_{off} and are relatively insensitive to k_{ff}, as is apparent from the results for 2 μM ADIFAB in Figure 1A. At higher ADIFAB concentrations (≥10 μM), a significant portion of FA initially bound to both hemileaflets of the vesicle ultimately binds to ADIFAB, and therefore, the time course of transfer reflects both k_{off} and k_{ff}. Thus, analysis of the dissociation time courses for ADIFAB at concentrations >1 μM and <10 μM, were used to determine k_{off}, while k_{ff} values were determined from the time courses at higher ADIFAB concentrations. The time course when

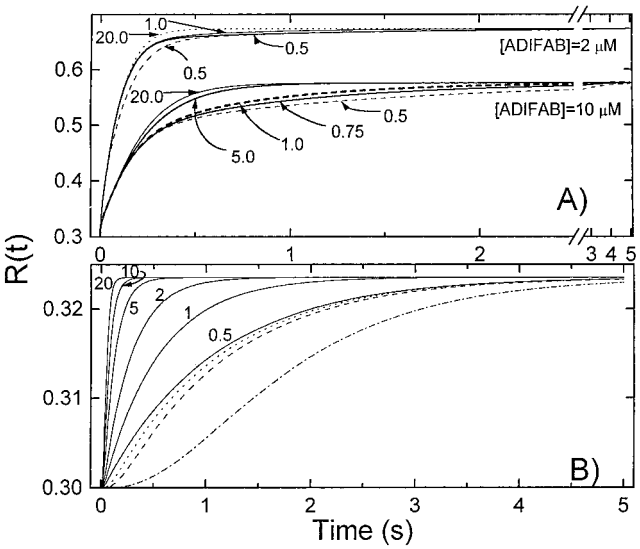

FIGURE 1: Simulated time courses of FA dissociation from and transport into vesicles. (A) Time courses for FA dissociation from lipid vesicles were calculated using eqs 1−5 to simulate measurements in which FA equilibrated with vesicles were rapidly mixed with ADIFAB. The upper set of curves for 2 μM ADIFAB were calculated with $k_{off} = 5.0\ s^{-1}$, with the exception of the dashed curve for which $k_{off} = 2.5\ s^{-1}$, k_{ff} (s^{-1}) values are as indicated on the figure. The lower set for 10 μM ADIFAB are all done using $k_{off} = 5.0\ s^{-1}$ and the indicated k_{ff} values (s^{-1}). (B) Transport time courses were calculated using eqs 1−5 to simulate measurements in which vesicles containing trapped ADIFAB were rapidly mixed with FA. All the solid curves are with $k_{off} = 5$ and the k_{ff} are varied between 0.5 and 20 as shown in the figure. The dotted, dashed, and dot-dashed curves are all with $k_{ff} = 0.5$ and with $k_{off} = 1.0$, 0.5, and 0.1, respectively.

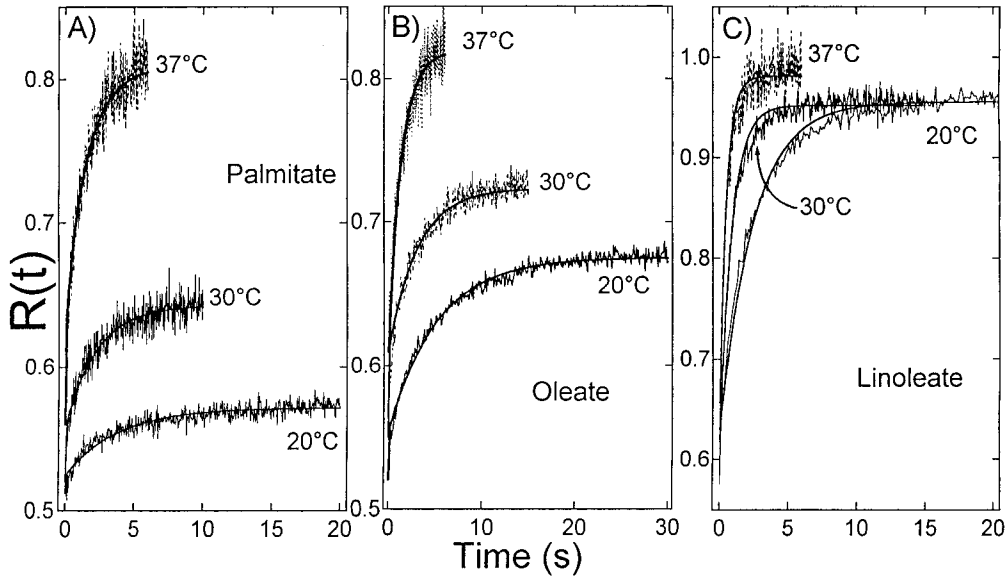

FIGURE 2: Transport of FA across GUV. GUV were prepared as EPC:cholesterol 2:1 LUV and contained ADIFAB trapped at a concentration of about 400 μM and the concentration of vesicles after mixing was 40 μM (EPC). (All concentrations quoted here and in the other figure legends are the values obtained after mixing in the stopped-flow observation chamber.) Time courses of the ratio of 505 to 432 nm ADIFAB fluorescence intensities ($R(t)$) following stopped flow mixing of FA vesicles, were measured at temperatures of 20, 30, and 37 °C. Increases in the equilibrium levels for palmitate and oleate with temperature, primarily reflect the increasing FA concentrations of these FA at the higher temperatures. This was done to ensure that the FFA were monomeric; at all temperatures, linoleate is more soluble than palmitate and oleate. Each trace is an average of more than five individual time courses. The solid lines through the data are best fits using $R(t)$ calculated with eq 8, as described in the Materials and Methods. (A) Results for palmitate at 20, 30, and 37 °C were obtained with total FA concentrations (μM) of 1.1, 2.4, and 5.2, respectively, for which fit results yielded k_{ff} values (s^{-1}) of 0.14, 0.24, and 0.34, respectively. (B) Results for oleate at 20, 30, and 37 °C were obtained with total FA concentrations (μM) of 2.0, 2.0, and 3.2, respectively, for which fit results yielded k_{ff} values (s^{-1}) of 0.10, 0.22, and 0.35, respectively. (C) Results for linoleate at 20, 30, and 37 °C were obtained with total FA concentrations (μM) of 7.7, 8.4, and 8.0, respectively, for which fit results yielded k_{ff} values (s^{-1}) of 0.23, 0.59, and 1.1, respectively.

$k_{ff} > k_{off}$ ($k_{ff} = 20$ s^{-1} in Figure 1A), being relatively independent of ADIFAB concentration, does not reveal the slow component of transfer that is observed at high ADIFAB concentrations when $k_{ff} < k_{off}$.

Time courses for transport of FA from the extra- to the intravesicular aqueous phase were simulated using numeric solutions of eqs 1−5 (Figure 1B). [Similar behavior was observed previously for simulations of the analytic solution, eq 8, for vesicle transport (Kleinfeld, 1995).] These results reveal that $R(t)$ increases from R_o and FFA is zero inside the vesicle at $t = 0$ and asymptotically approaches an equilibrium value equal to the [FFA] predicted from membrane partition. For $k_{ff} < k_{off}$, these simulations predict that the time courses will depend sensitively on k_{ff} but only weakly on k_{off}. Thus, an accurate determination of k_{ff} can be obtained with only a rough estimate of the k_{off} value. Although the equilibrium R value will increase with increasing FA_T and/or decreasing vesicle concentration, in contrast to the time course for dissociation, the shape and therefore the k_{ff} dependence of the transport time courses is independent of FA_T, vesicle, and ADIFAB concentrations. For $k_{off} < k_{ff}$, the simulations reveal a considerable sensitivity to k_{off} (dot and dashed curves in Figure 1B), and moreover, the shape of the time course reveals a pronounced inflection at initial times that is distinctly different from the $k_{ff} < k_{off}$ case.

Monitoring Transbilayer Transfer of AOFA Using Pyranine-Containing Vesicles. The transbilayer flip-flop of FA was also monitored by measuring the quenching of the fluorescence of trapped pyranine that occurs when FA increase the pH of the inner aqueous compartment upon transfer from the outer to the inner leaflet (Kamp et al., 1993, 1995; Kleinfeld et al., 1997b) We have used this approach in the present study to obtain an assessment of the time course for flip-flop in GUV that is independent of ADIFAB. Pyranine concentrations and buffer conditions were described previously (Kleinfeld et al., 1997b). Also, as discussed previously (Kleinfeld et al., 1997b), time constants (τ) from single exponential fits rather than k_{ff} were determined because the various parameters required for converting τ to k_{ff} were not specifically determined.

RESULTS

The Time for Transport of Long-Chain FA across GUV Composed of Egg Phosphatidylcholine and Cholesterol Is on the Order of Seconds. Transport of long-chain FA from the external aqueous phase, across the lipid bilayer, and into the inner aqueous phase of lipid vesicles was measured by stopped-flow mixing FA with lipid vesicles containing ADIFAB. Because the ratio of ADIFAB fluorescence [$R(t)$] is a sensitive and specific measure of the FFA concentration (Richieri et al., 1992, 1997; Richieri & Kleinfeld, 1995a,b), these transport measurements provide the time course for [FFA_i] following stopped-flow mixing. Figure 2 shows results obtained for the transport of palmitate, oleate, and linoleate across GUV composed of 2:1 EPC:cholesterol at temperatures of 20, 30, and 37 °C. These results are typical of FA transport across EPC:cholesterol GUV and reveal that the times required for the [FFA] to reach equilibrium inside the vesicles range from about 2 to more than 30 s, depending upon FA type and temperature. In particular, rates of transport are slowest for oleate and fastest (about 3-fold greater) for linoleate. Moreover, for all three FA, rates of transport increase about 3-fold as the temperature is increased from 20 to 37 °C.

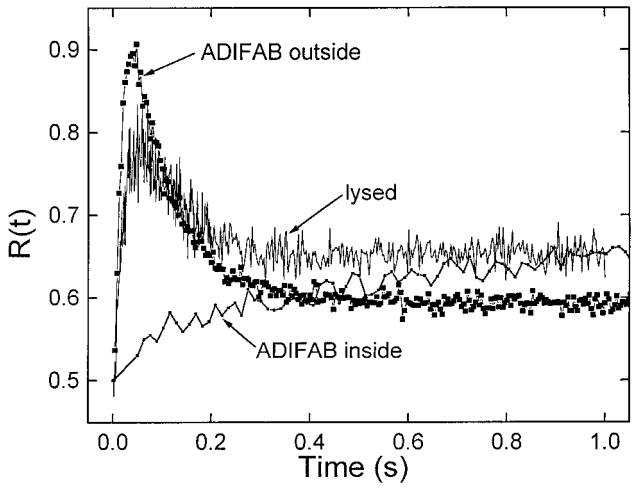

FIGURE 3: The lipid membrane imposes a barrier that slows FA transport. These measurements of the time courses were done by stopped-flow mixing of GUV composed of EPC:cholesterol 3:1 and oleate at 37 °C. $R(t)$ is the ADIFAB intensity ratio as in Figure 2. The lower curve labeled "ADIFAB inside" illustrates the slow time course for oleate transport across intact vesicles as in Figure 2. For the data labeled "lysed", these same vesicles were first lysed by a 20:1 dilution in hypotonic buffer, return to isotonicity and then stopped-flow mixed with oleate. The data labeled "ADIFAB outside" are intact vesicles to which ADIFAB was added after vesicle formation.

The Lipid Bilayer Membrane Is the Rate-Limiting Barrier for FA Transport Across GUV. To demonstrate that the rate of transport is limited by vesicle membrane, we compared time courses for intact vesicles with ones that were lysed, either by osmotic shock or by treatment with digitonin. These measurements at 37 °C revealed that for lysed vesicles the ADIFAB fluorescence ratio peaks in less than 50 ms and then decays to equilibrium in less than 200 ms (Figure 3). In contrast, for intact vesicles with entrapped ADIFAB, the time course exhibits the same slow (>5 s) monotonic approach to equilibrium observed for transport through intact vesicles as shown, for example, in Figure 2. The rapid increase in R observed with the lysed vesicles reflects the binding of FA to ADIFAB that was released from the vesicles by lysis. Direct measurements of FFA binding to ADIFAB are consistent with this rapid time course (Richieri et al., 1996a). The R value exhibits a peak at these early times because the FFA concentration just after mixing exceeds the equilibrium value. The relatively slow decay toward equilibrium, from the peak value, reflects the rate of FA dissociation from ADIFAB and partition into the membrane lipid. Support for this explanation is provided by the similar time course obtained when intact vesicles and extravesicular ADIFAB are mixed with FA, as also shown in Figure 3. These results indicate that the time needed for FA transport across GUV reflects the barrier imposed by the lipid bilayer and is not due, for example, to a slow rate of dissociation from FA aggregates. Dissociation from FA aggregates, which form at concentrations higher than used in this study (Richieri et al., 1992), is significantly slower than the time courses shown in Figure 2 (Kleinfeld et al., 1997b, and data not shown).

Rates for FA Dissociation from and Binding to EPC:Cholesterol GUV Are Faster Than Transport Rates. Although the results of Figure 2 demonstrate that transport of long-chain FA across EPC:cholesterol GUV requires seconds and that the lipid bilayer membrane is the barrier to transport,

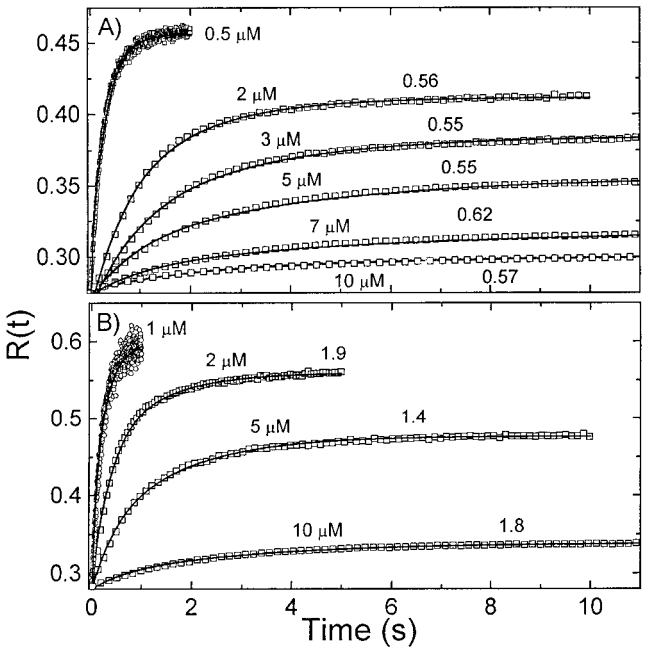

FIGURE 4: Time courses for FA dissociation from GUV. GUV composed of EPC:cholesterol 3:1 at a concentration of 50 uM EPC and 5 μM FA were stopped-flow mixed with ADIFAB at concentrations between 0.5 and 10 μM. These time courses are averages of at least three separate scans of the ADIFAB fluorescence ratio [$R(t)$, as in Figure 2]; only a subset of the data points are shown so that both data and fits are visible. The solid lines through the data (symbols) are fits using eqs 1−5 as described in the Materials and Methods. Each time course is denoted with the ADIFAB concentration and the best fit values for k_{off} in inverse seconds. (A) These time courses were determined for oleate−vesicle complexes at 37 °C. Fit values for k_{ff} (in inverse seconds) obtained in these analyses are 0.40, 0.18, 0.20, 0.16, and 0.20 for 2, 3, 5, 7, and 10 μM ADIFAB, respectively. (B) Time courses for linoleate−vesicle complexes at 20 °C. Fit values for k_{ff} (in inverse seconds) obtained in these analyses are 0.8, 0.6, and 0.4 for 2, 5, and 10 μM ADIFAB, respectively.

they do not indicate which step is rate limiting. To do this, we determined, separately, the rate constants for dissociation from the bilayer (k_{off}), binding to the vesicle surface (k_{on}), and flip-flop (k_{ff}). We determined k_{off} by measuring the time course for transfer of FA from vesicles to extravesicular ADIFAB, as described in the Materials and Methods. Results of these measurements show that $R(t)$ increases monotonically after mixing and that the time required to reach equilibrium increases with increasing ADIFAB concentration (Figure 4). The results also indicate that transfer rates for oleate and palmitate are similar, but about 3−4-fold slower than for linoleate, and for all three FA the rates increase about 2-fold between 20 and 37 °C (Table 2).

As discussed in the Materials and Methods, simulations using the kinetic model of eqs 1−5 predict that the time for transfer of FA from vesicle to ADIFAB should increase with increasing ADIFAB concentration and that the transfer time course should be sensitive to k_{off} for ADIFAB concentrations ≥2 μM (Figure 1). We therefore analyzed the measured time courses for dissociation using eqs 1−5, typical results are shown as solid lines through the data of Figure 4. These fits reveal unique values for k_{off} at ADIFAB concentrations ≥2 μM. In the examples shown in Figure 4, k_{off} values of 0.57 ± 0.03 s^{-1} and 1.7 ± 0.3 s^{-1} for oleate and linoleate, respectively, were obtained for ADIFAB concentrations between 2 and 10 μM. Analysis of all GUV measurements reveals k_{off} values that range from about 0.2 to 7 s^{-1},

Table 2: Rate Constants for Dissociation from GUV[a]

fatty acid	20 °C	30 °C	37 °C
	EPC:cholesterol		
oleate	0.3		0.7
palmitate	0.4		0.8
linoleate	1.2		2.5
	EPC		
oleate	0.5	0.8	1.5
palmitate	0.5		1.7
linoleate	2.3	3.5	7.3

[a] k_{off} is in units of inverse seconds. For EPC:cholesterol GUV, the values are averages of results for at least two preparations of vesicles composed of EPC:cholesterol between 2:1 and 3:1 and for each vesicle preparation measurements were done for at least four different ADIFAB concentrations so that the number of independent experiments for each entry in the table ranged between 5 and 22. For EPC GUV the number of independent experiments ranged between 2 and 20. The k_{off} values determined from the analysis (see Materials and Methods and Figure 4) of each of the separate time courses (which are each averages of at least five separate traces) were averaged and the standard deviations of the distribution of k_{off} values for each entry in the table was approximately 0.1 and 0.2 s^{-1} for EPC:cholesterol and EPC GUV, respectively.

Table 3: Rate Constants (k_{on}) for FA Binding to EPC:Cholesterol GUV[a]

fatty acid	20 °C	37 °C
oleate	1.0	2.8
palmitate	2.5	4.0
linoleate	1.8	3.8

[a] Values were calculated as $k_{on} = k_{off}K_p$ using k_{off} values of Table 2 and K_p values indicated in the Materials and Methods, and are in units of 1×10^{-5} M^{-1} s^{-1}. The uncertainties in these values, estimated using the uncertainties for k_{off} in Table 2 and 10% for K_p, which is consistent with our previous estimates (Anel et al., 1993) and the current measurements (Materials and Methods), range from about 30% for oleate at 20 °C to about 10% for linoleate at 37 °C.

depending upon temperature, FA type, and vesicle composition (Table 2). In particular, k_{off} values are 3−5-fold greater for linoleate than oleate and palmitate, increase about 2−3-fold upon raising the temperature from 20 to 37 °C for all three FA, and are 2−3-fold greater for EPC than vesicles containing cholesterol, at EPC:cholesterol values between 2 and 3:1.

The rate constant for binding to the vesicle surface (k_{on}) can be calculated from k_{off} and K_p, as indicated in the Materials and Methods. These values were found to range from about 1×10^5 M^{-1} s^{-1} for oleate at 20 °C to about 1×10^6 M^{-1} s^{-1} for linoleate at 37 °C (Table 3). Using these rate constants, we estimate the *rate* of FA binding, as k_{on} [Lipid], to be greater than 5 s^{-1}. This is substantially faster than the rate of transport, and therefore the on-step is not rate limiting.

Flip-Flop Is the Rate-Limiting Step for Long-Chain FA Transport across GUV. The above results indicate that both the off- and on-steps are faster than the rates of transport across EPC:cholesterol GUV. Thus, the rate-limiting step for long-chain FA transport is transbilayer flip-flop. Flip-flop rate constants were determined by fitting the time courses for transport with solutions to eqs 1−5, as described in the Materials and Methods. Results of this analysis, as represented, for example, by the solid lines through the transport data of Figure 2, provide unique values for k_{ff}. Moreover, as discussed in the Materials and Methods and the figure legend of Figure 2, the k_{ff} values are relatively insensitive to k_{off} when $k_{ff} < k_{off}$. [In addition to the direct measurements of k_{off}, the lack of an inflection in the transport time course at early times also provides support that $k_{ff} < k_{off}$ (Figure 1B).] Flip-flop rate constants determined by this analysis range from about 0.1 s^{-1} for oleate at 20 °C to about 1 s^{-1}, for linoleate at 37 °C. Linoleate k_{ff} values were consistently about 3-fold greater than those for oleate, and for all three FA, k_{ff} values increase about 3-fold between 20 and 37 °C (Table 4).

Table 4: Flip-Flop Rate Constants from FA Transport in EPC:Cholesterol GUV[a]

fatty acid	20 °C	30 °C	37 °C
oleate	0.1	0.2	0.3
palmitate	0.2	0.3	0.5
linoleate	0.3	0.6	1.0

[a] Values for k_{ff} are in units of inverse seconds. For oleate and linoleate, k_{ff} is the average of results of more than three separate preparations of vesicles composed of EPC:cholesterol between 2:1 and 3:1, while for palmitate k_{ff} is for vesicles composed of EPC:cholesterol 2:1 only. For each preparation, FA, and temperature, time courses such as those in Figure 2 (which are averages of at least five separate traces) were measured for at least three different FA concentrations and in many cases more than once for each concentration. The number of independent experiments for each entry in the table ranged between 10 and 28. The k_{ff} values were determined from fits to each one of these time courses with either the solutions to eqs 1−5 and/or eq 8 and with k_{off} values ≥ those in Table 2 (k_{off} values used for the 30 °C were ≥ extrapolations of Table 2 values). The values given in the table are the averages of all of these determinations and the standard deviations were between 0.05 and 0.1 s^{-1}.

Table 5: Flip-Flop Rate Constants from EPC:Cholesterol GUV Dissociation Measurements[a]

fatty acid	20 °C	37 °C
oleate	0.1	0.3
palmitate	0.1	0.3
linoleate	0.5	1.5

[a] Values of k_{ff} are in units of inverse seconds and are averages of results with vesicles composed of EPC:cholesterol between 2:1 and 3:1 as described for Table 2. The k_{ff} values were determined by fiting time courses for dissociation with solutions to eqs 1−5 as described for the results in Figure 4 and in the Materials and Methods. Estimated standard deviations for these determinations are about 0.2 s^{-1}.

In addition, to obtaining k_{ff} values directly from the transport measurements, we also determined k_{ff} from analysis of the time courses for FA transfer from vesicles to ADIFAB. As described in the Materials and Methods, analysis of these time courses should be sensitive to k_{ff}, especially at the highest ADIFAB concentrations. Values obtained from this analysis of the GUV data are in good agreement with those determined directly from the transport measurements (Table 5).

Time Course of Pyranine Fluorescence in EPC:Cholesterol GUV Is Also Consistent with Flip-Flop Times on the Order of Seconds. The above results, obtained using ADIFAB to detect transport of FA, reveal that long-chain FA flip-flop across GUV occurs with time constants between about 1 and 10 s. To confirm these results, we also measured the time course for quenching of pyranine fluorescence as the internal pH is reduced upon flip-flop of the protonated FA (Kamp et al., 1995; Kleinfeld et al., 1997b). In these measurements, GUV composed of EPC and cholesterol at 3:1 mole ratio with trapped pyranine were mixed with oleate

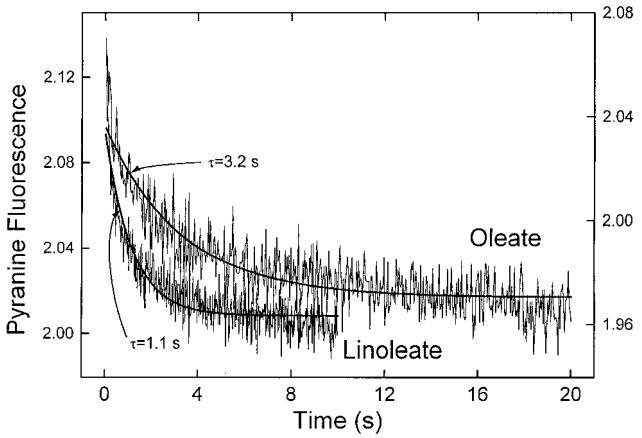

FIGURE 5: Time courses of FA mediated quenching of pyranine fluorescence in GUV. GUV were prepared with EPC:cholesterol 3:1 and contained 500 μM. These measurements were done at 20 °C with 3 μM oleate or 5 μM linoleate and 50 μM GUV in the final mixture following stopped-flow mixing. The solid curves through the data are single exponential fits with time constants as indicated.

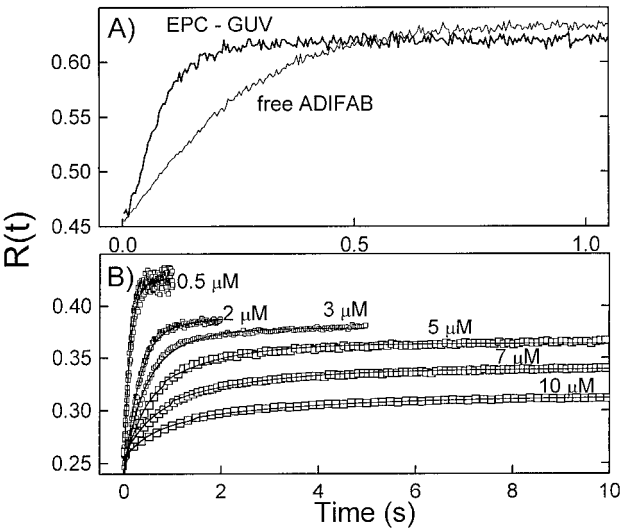

FIGURE 6: Time courses for FA transport across and dissociation from EPC-GUV. GUV composed of EPC were prepared either with (A) or without (B) trapped ADIFAB (about 400 μM). (A) Transport measurements at 20 °C done using vesicles (50 μM) containing trapped ADIFAB that were stopped-flow mixed with 2 μM oleate (thicker line) and stopped-flow mixing of ADIFAB (0.1 μM, equivalent to the concentration of vesicle trapped ADIFAB relative to the total aqueous volume) and 2 μM oleate. (B) Oleate dissociation measured at 37 °C from 50 μM vesicles equilibrated with 2 μM oleate and mixed with ADIFAB at concentrations between 0.5 and 10 μM. Solid curves through the data are best fits using eqs 1−5 and yield the following k_{off}, k_{ff} values (s^{-1}): 1.8, 0.6; 1.8, 1.6; 1.6, 0.6; 1.8, 0.5; and 1.4, 0.3 for 2, 3, 5, 7, and 10 μM ADIFAB, respectively.

or linoleate and the decay of pyranine fluorescence was monitored at temperatures between 10 and 37 °C. The results yield time constants of about 1 and 3 s for linoleate and oleate, respectively at 20 °C (Figure 5). These times are reasonably consistent with the results obtained using ADIFAB but are 50−150-fold slower than the values reported previously for LUV (Kamp et al., 1995).

Transport across EPC GUV. The above results demonstrate that times for transport of long-chain FA across GUV composed of EPC:cholesterol is on the order of seconds. In contrast, similar measurements done using GUV composed of EPC, without cholesterol, give the appearance of very rapid transport. As Figure 6 indicates, the time course for oleate mixed with these vesicles reveals a time constant of about 80 ms at 20 °C and, moreover, the time courses are also independent of the molecular species of FA (data not shown). Several factors suggest that this rate does not reflect transport across an intact EPC membrane. First, the rate of dissociation of oleate from the bilayer surface is about 0.5 s^{-1} for these vesicles (Figure 6B and Table 2), and therefore, even if the time for flip-flop across these vesicles were extremely fast, the transport time should be slower than about 2 s.

Second, surprisingly the rate of transport for EPC GUV is *faster* than the binding of FA to free ADIFAB (Figure 6A), which is in contrast to the results for EPC:cholesterol GUV (Figure 3). (Rates are slower in Figure 6A than Figure 3 because the Figure 3 data was obtained at 37 °C.) This presumably reflects FA reacting with the high concentration of trapped ADIFAB within the vesicles (about 400 μM relative to the internal aqueous compartment) and implies that the bilayer is able to retain ADIFAB but presents no barrier to the FA. This can only occur if the FA does not insert into the bilayer, because otherwise the rate would be limited by dissociation and suggests the formation of transient "pores", during stopped-flow mixing with FA, sufficient to allow passage of FA but not ADIFAB. That the integrity of these vesicles is affected by stopped-flow mixing is apparent from measurements done using EPC GUV that were collected from the outflow of the stopped-flow device after mixing with buffer alone. These vesicles (but not EPC:cholesterol GUV) reveal *slower* transport rates than "unused" vesicles and reveal an increase (more than 40%) in accessibility to Na_2MoO_4 quenching, relative to unused vesicles (data not shown). Moreover, these vesicles are intact before stopped-flow mixing because (data not shown) (1) the concentration of ADIFAB associated with these vesicles is consistent with a high degree of trapping efficiency, (2) the trapped ADIFAB is not quenched significantly by Na_2MoO_4, and (3) the trapped ADIFAB is not cleaved by trypsin. Finally, rate constants for flip-flop determined from measurements of dissociation yield k_{ff} values inconsistent with rapid flip-flop (Figure 6B). As shown in Figure 6B, dissociation of oleate from these vesicles reveals a similar pattern with ADIFAB concentration as for EPC:cholesterol vesicles, indicative of slow flip-flop relative to the rate of dissociation (Figure 1A). Analysis of the EPC-GUV dissociation time courses with eqs 1−5 yields, for oleate at 37 °C, a k_{ff} of about 0.5 s^{-1} (Figure 6B).

We conclude that, during stopped-flow mixing with FA, the permeability of EPC GUV increase transiently, thereby allowing FA in the extravesicular aqueous phase rapid access to the internal aqueous compartment. However, when FA are pre-equilibrated with the membrane, their transbilayer movement is rate limited by slow flip-flop. In part, the increase in permeability is probably due to the shear forces developed during mixing because stopped-flow mixing without FA causes leakage of ADIFAB from EPC GUV (but not from EPC-cholesterol GUV). In addition, we speculate that, because of slow FA flip-flop, rapid partition of FA into the bilayer will result in a transient asymmetry between the outer and inner hemileaflet areas, and this may compromise the integrity of EPC GUV.

Transport of Long-Chain FA across LUV. Long-chain FA transport was also measured across unilamellar vesicles

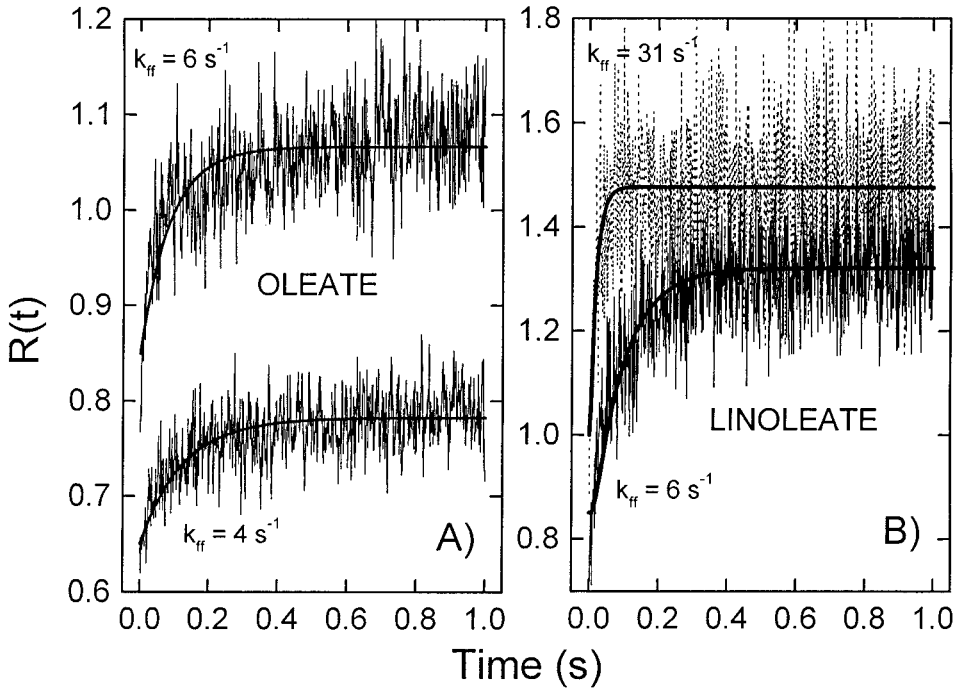

FIGURE 7: Time courses for transport of FA across EPC:cholesterol LUV. These results show that transport across LUV is complete within about 50−400 ms, depending upon temperature and FA-type. LUV (75 μM) were loaded with about 400 μM ADIFAB. (A) LUV composed of EPC:cholesterol, 3:1 were stopped-flow mixed with 3 μM and 5 μM oleate at 20 and 37 °C, respectively. Solid lines through the data are best fit solutions of eqs 1−5 and yield k_{ff} values of 4 and 6 s^{-1} for 20 and 37 °C, respectively. (B) LUV composed of EPC:cholesterol, 2:1 were stopped-flow mixed with about 10 μM linoleate at 20 and 37 °C, respectively. Solid lines through the data are best fit solutions of eqs 1−5 and yield k_{ff} values of 6 and 30 s^{-1} for 20 and 37 °C, respectively.

prepared by extrusion (LUV) that are less than half the diameter of the GUV prepared by detergent dialysis (Hope et al., 1985; Marassi et al., 1993). Measurements of oleate and linoleate transport were done using LUV composed of EPC:cholesterol between 2:1 and 3:1. Results of these measurements reveal that FA transport across these vesicles is complete within times between 50 and 400 ms, depending on temperature and FA type (Figure 7), which is considerably faster than for the GUV.

To determine the rate-limiting step for transport, we measured, as for GUV above, the time course of FA transfer from LUV to ADIFAB. Results of these measurements reveal a similar dependence on ADIFAB concentration but faster transfer times than for GUV (Figure 8). Similar results were also obtained for FA dissociation from EPC LUV (data not shown). Analysis of the dissociation time courses using eqs 1−5 yields k_{off} values that range from about 4 s^{-1} for oleate at 20 °C to 40 s^{-1} for linoleate at 37 °C (Table 6). Thus, for these vesicles, as well as for GUV, the off-step is not rate limiting for transport. The binding step (k_{on}) is also not rate limiting, and calculated k_{on} values range from about 2×10^6 M^{-1} s^{-1} for oleate at 20 °C to about 6×10^6 M^{-1} s^{-1} for linoleate at 37 °C, which indicates that the rate of FA binding to these vesicles is greater than 100 s^{-1}.

Flip-flop is, therefore, also the rate-limiting step for transport across LUV. Flip-flop rate constants determined from the time courses of transport across EPC:cholesterol LUV, using eqs 1−5, ranged from less than 3 s^{-1} for oleate at 20 °C to about 15 s^{-1} for linoleate at 37 °C. In general, k_{ff} values depend similarly on temperature and FA type as for GUV, although the magnitudes are more than 10-fold greater for LUV than for GUV (Table 7).

DISCUSSION

In this study, we measured the transport of long-chain FA from the aqueous phase on one side of lipid bilayer vesicles to the aqueous phase on the opposite side. These measurements were done using ADIFAB, the fluorescent probe that can accurately quantitate the concentration of long chain native FA in the aqueous phase. As far as we are aware, this is the first report, with the exception of our preliminary studies (Kleinfeld, 1995; Kleinfeld et al., 1997a), of transmembrane *transport* of the long-chain FA. The results of these measurements reveal that times for transport of FA range from about 70 ms to 10 s, depending on vesicle size, FA type, and temperature. We also determined the rates of FA dissociation and binding for these vesicles, and in all cases, the results indicate that transbilayer flip-flop is the rate-limiting step for transport. In particular, rates of flip-flop determined using ADIFAB range between 0.1 and 1.0 s^{-1} for GUV composed of EPC:cholesterol (times for oleate flip-flop were >3 s), and these rates were confirmed using pyranine to detect flip-flop of the neutral species of FA. Flip-flop rates were found to be ≥10-fold greater in LUV than in GUV, raising the possibility that in cell size membranes transport rates of the physiologically important FA through the lipid phase of the membrane may be too slow to support physiologically required transport rates.

Comparison with Previous Studies of FA Flip-Flop. Previous studies using pyranine trapped within lipid vesicles to detect flip-flop rates for long-chain natural FA in small unilamellar vesicles (SUV ≈ 200 Å diameter) reported rates that were too fast (time constant < 5 ms) to be resolved by stopped-flow fluorometry (Kamp et al., 1995). Using the larger vesicles formed by extrusion (∼1000 Å diameter) Kamp et al. (1995) found slower, but still quite rapid, flip-

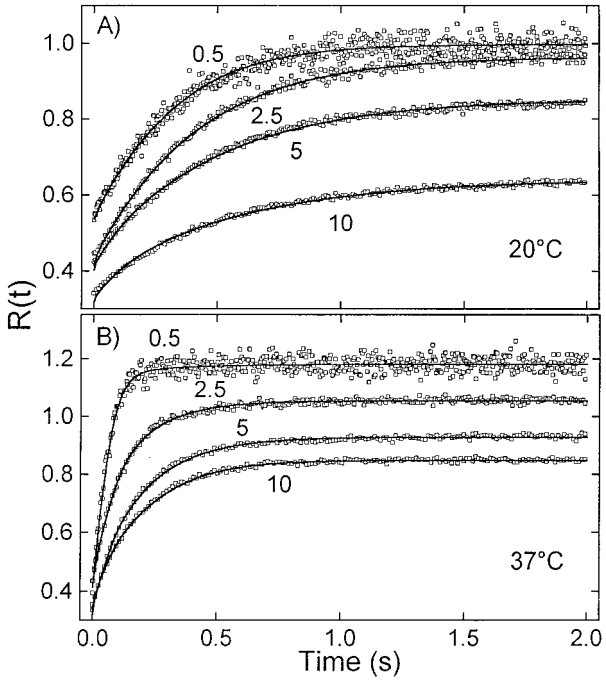

FIGURE 8: Time courses for FA dissociation from LUV. LUV composed of EPC:cholesterol 2:1 at a concentration of 40 μM EPC and 5 μM oleate were stopped-flow mixed with ADIFAB at concentrations between 0.5 and 10 μM. These time courses are averages of at least three separate scans of $R(t)$; only a subset of the data points are shown so that both data and fits are visible. The solid lines through the data (symbols) are fits using eqs 1−5 as described in the Materials and Methods. Each time course is denoted with the ADIFAB concentration. (A) These time courses were determined for oleate−vesicle complexes at 20 °C. Fit values for k_{off} (in inverse seconds) obtained from these analyses were: 5.5, 6.9, and 8.2 for 2.5, 5, and 10 μM ADIFAB, respectively, and k_{ff} values were about 2 s^{-1}. (B) Time courses at 37 °C. Fit values for k_{off} (in inverse seconds) obtained from these analyses were 15, 15, and 18 for 2, 5, and 10 μM ADIFAB, respectively, and k_{ff} values were about 5 s^{-1}.

Table 6: Dissociation rate constants from EPC:cholesterol LUV[a]

fatty acid	20 °C	30 °C	37 °C
oleate	4	6	10
palmitate	2	5	8
linoleate	8	21	40

[a] k_{off} are in units of inverse seconds and values are averages of results for two different preparations of vesicles composed of EPC:cholesterol of 2:1 and 3:1, and for each vesicle preparation, measurements were done for at least three different ADIFAB concentrations so that the number of independent experiments for each entry in the table ranged between 10 and 16. Although not used in these averages, k_{off} was also determined for EPC LUV and yieled similar results. The k_{off} values were determined from each experiment as described for Table 2 and Figure 8, and the standard deviations were estimated from the distribution of k_{off} values to be about 20% of k_{off}.

flop times of about 20 ms, from which they calculated a flip-flop rate constant for unionized FA of 15 s^{-1}. [The flip-flop rate constants for ionized oleate is about 4×10^{-4} s^{-1} or about 4×10^4-fold smaller than these values for the unionized FA (Gutknecht, 1988).] Moreover, these rates were found to be similar, within a factor of 2, for native FA with chain lengths between 12 and 18 carbons and for the long-chain anthroyloxy FA (AOFA).

Comparative results from the present study for vesicles formed by extrusion (LUV) reveal transport times of >200 ms and k_{ff} values (3 s^{-1}) for oleate at 20 °C (Table 7) that

Table 7: Flip-Flop Rate Constants in EPC:Cholesterol LUV[a]

fatty acid	20 °C	30 °C	37 °C
oleate	3	5	6
linoleate	5		15

[a] Values for k_{ff} are in units of inverse seconds. These values are averages of results for oleate in three separate preparations of vesicles composed of EPC:cholesterol between 2:1 and 3:1 and for linoleate in vesicles composed of EPC:cholesterol 2:1. The number of independent experiments (as described in Tables 2 and 4) for each entry in the table ranged between 3 and 9. The k_{ff} values were determined as described in Table 4 and the standard deviations from the distribution of k_{ff} values was about 1 s^{-1}.

are about 4-fold slower and smaller, respectively, than those of Kamp et al. (1995). We have also recently investigated the issue of AOFA flip-flop in SUV and LUV using the pyranine method of Kamp et al. (1995) as well as a separate method involving energy transfer between the AOFA and carboxyfluorescein trapped within the vesicles (Kleinfeld et al., 1997b). In contrast to Kamp et al. (1995) but consistent with our earlier studies of AOFA (Storch & Kleinfeld, 1986; Kleinfeld & Storch, 1993), both types of measurements yielded flip-flop times on the order of minutes for the long-chain AOFA and more than 50-fold faster rates for an 11 carbon chain AOFA. We conclude, therefore, that flip-flop of long-chain native and AO-labeled FA across LUV is rate limiting, but that the rates for the AOFA are about 1000-fold slower than for the native FA.

These results emphasize that rate constants for FA flip-flop across membranes are extremely sensitive to both the nature of the FA as well as the membrane. Assessment of the role of the lipid phase in FA transport across biological membranes should therefore be done using native FA and bilayers whose radius of curvature and lipid composition more accurately represents the biological membrane. In this regard, it is significant that flip-flop of long-chain FA across GUV (>2000 Å) composed of EPC:cholesterol requires times of several seconds (Table 4) while flip-flop of short chain FA (octanoate) across soybean PC SUV occurs in 0.000 06 s (Srivastava et al., 1995). Moreover, previous studies of AOFA (Storch & Kleinfeld, 1986; Kleinfeld & Storch, 1993; Kleinfeld et al., 1997b) and native FA (Kamp et al., 1995; Kleinfeld, 1995) also support this trend of decreasing flip-flop rate constants with increasing FA and vesicle size.

Our results also indicate that k_{off} values are significantly smaller (about 10-fold) for GUV compared to LUV (Tables 2 and 7). However, rates of FA dissociation, measured using FA transfer between pyranine containing vesicles, have been reported to be similar for SUV and LUV (Zhang et al., 1996). Indeed the k_{off} values for EPC SUV found for palmitate, oleate, and linoleate, 8, 1.8, and 12 s^{-1} respectively, at 24 °C, are similar to the values found in the present study for LUV (Table 6). Studies of Massey et al. (1997), however, reveal k_{off} values for 1-palmitoyl-2-oeoyl-*sn*-glycero-3-phosphocholine SUV that are more than 5-fold greater than those of Zhang et al. (1996). Moreover, studies of the transfer of a variety of other amphipathic molecules between lipid vesicles are consistent with decreasing rates of dissociation with increasing vesicle dimensions (Letizia & Phillips, 1991; Kleinfeld & Storch, 1993; Zucker et al., 1994; Noy et al., 1995). We conclude, therefore, that rates of dissociation as well as flip-flop, decrease with increasing vesicle diameter.

Table 8: Eyring Rate Theory Analysis of Flip-Flop Rate Constants in EPC:Cholesterol GUV[a]

fatty acid	$\Delta G^{\ddagger\circ}$	$\Delta H^{\ddagger\circ}$	$-T\Delta S^{\ddagger\circ}$
oleate	18.7	11.1	7.5
palmitate	18.4	9.0	9.4
linoleate	18.1	12.4	5.6

[a] Values for the activtion thermodynamic parameters $\Delta G^{\ddagger\circ}$,$\Delta H^{\ddagger\circ}$, and $-T\Delta S^{\ddagger\circ}$ are in kilocalories per mole and were determined from the k_{ff} values of Table 4 using Eyring rate theory as described previously (Doody et al., 1980; Kleinfeld & Storch, 1993).

Characteristics of FA Transport across Vesicles and the Mechanism of Flip-Flop in Lipid Bilayers. Comparison of the results obtained for native and AOFA provides insight about the mechanism by which FA may undergo flip-flop between the hemileaflets of the bilayer. Flip-flop of the long-chain AOFA is 2−3 orders of magnitude slower than for the native FA, and the long (16 carbon)-chain AOFA is at least 50-fold slower than for the shorter (11 carbon) AOFA (Storch & Kleinfeld, 1986; Kleinfeld & Storch, 1993, this study). These results indicate that the flip-flop rate constant is inversely related to the size of the FA and suggests that the rate-limiting step for FA movement across the bilayer may involve the formation of a free volume sufficiently large to enclose the FA. This mechanism has been suggested for the movement of other nonelectrolytes across lipid membranes and, in particular, has been used to explain the steep size dependence of permeability (Stein, 1986; Bassolino-Klimas et al., 1993). Much slower flip-flop rates for the AOFA, whose molecular weights are almost 2-fold greater than the corresponding unlabeled FA (native), is consistent with this idea, and the greater k_{ff} for linoleate as compared to palmitate and oleate may also be a reflection this mechanism. Linoleate's additional double bond results in a greater degree of disorder of the acyl chains of the bilayer's phospholipids (Anel et al., 1993), which might increase the rate of formation of a free volume cavity within the bilayer.

Eyring rate theory analysis of the k_{ff} values for EPC: cholesterol reveals that the activation barrier is composed of substantial admixtures of enthalpic and entropic contributions (Table 8). The enthalpic components of the activation free energy are, given the 1−2 kcal/mol uncertainties for these values, reasonably constant for the three FA, with the smaller barrier for linoleate possibly due to its smaller entropic component. We speculate that the enthalpic portion of the flip-flop barrier may reflect more the cost of burying the polar portion of the FA while the entropic part may more reflect the cost of cavity formation. Our previous results for 12-AO-stearate flip-flop across EPC GUV (Kleinfeld & Storch, 1993), indicating much larger $-T\Delta S^{\ddagger\circ}$ values (∼18 kcal/mol) than for the native FA (5−9 kcal/mol) (Table 8) is roughly consistent with this notion.

Additional evidence consistent with a mechanism involving defect formation within the bilayer as a rate-limiting step for transbilayer flip-flop is the decrease in rate with increasing radius of curvature and with cholesterol content. Cavity formation may be promoted by phospholipid packing defects and these will likely increase with increasing mismatch of bilayer areas. Differences in outer to inner hemileaflet areas are 90% in SUVs (200 Å diameter), 15% in LUV (∼1000 Å diameter), and less than 8% in GUV (>2000 Å diameter). Qualitatively, the increase in flip-flop rate constants follows this trend: rates for both native (Kamp et al., 1995) and AOFA (Storch & Kleinfeld, 1986; Kleinfeld & Storch, 1993) are fastest in SUV, intermediate (Kleinfeld et al., 1997b) in LUV, and slowest in GUV (Kleinfeld & Storch, 1993; Table 4).

Metabolic Requirements and Transport Rates of Long-Chain FA across the Lipid Phase of Cell Membranes. The results of this study indicate that transport of long-chain FA across lipid bilayer membranes requires several seconds and that flip-flop is rate limiting. Whether this rate of transport is slow is meaningful only with respect to rates of transport across cell membranes. Cellular transport rates can be estimated from rates of total FA metabolism, primarily β-oxidation and FA esterification, that have been determined in adult rat heart myocytes in several studies (Glatz et al., 1984; Bielefeld et al., 1985; Forsey et al., 1987; Linssen et al., 1990; Lopaschuk et al., 1990). We will estimate the transport rate constants from the measured metabolic rates by expressing the flux of FA across a cell membrane, using the Einstein relationship, $1/2\lambda^2/t$ for the diffusion coefficient D, and identifying $1/t$ as the transport rate constant as [see, for example, Stein (1986)].

$$J = {}^1/_2\, \lambda A K_p \Delta C k_t \qquad (6)$$

in which J is the FA flux (mol/s) across a cell membrane of area A, driven by a concentration difference ΔC ($= C_o - C_i$, where C_o and C_i are the aqueous phase concentrations of FA in the region just outside and inside of the plasma membrane, respectively), K_p is the membrane/water partition coefficient, λ is the thickness of the membrane, and k_t is the transport rate constant. In the following estimates, we use a value for λ of 40×10^{-8} cm (Mason & Huang, 1978) and a K_p value for oleate or palmitate of 4×10^5 (Anel et al., 1993; this study). Values for the myocyte surface area A (4000 μm^2) and its volume (8000 μm^3) were obtained from the study of (Anversa et al., 1980) and a value of 75×10^6 myocytes/g of wet tissue from (Vork et al., 1993). Measurements of palmitate or oleate oxidation have been done using isolated suspensions of cardiac myocytes as well as whole tissue and the results of these measurements yield rates that range from about 2×10^{-5} to about 18×10^{-5} pmol/cell/s (Glatz et al., 1984; Bielefeld et al., 1985; Forsey et al., 1987; Linssen et al., 1990; Lopaschuk et al., 1990), where the value of 75×10^6 myocytes/g of wet tissue was used to convert to a per cell value. The value for ΔC is unknown, and no measurements have been done to determine intracellular FFA levels, although FFA_i has been estimated to be 3 nM in cardiac myocytes (Vork et al., 1993). We have previously determined that serum FFA levels are 7 nM under normal physiologic conditions (Richieri & Kleinfeld, 1995b), although it is unclear how this value relates to the actual extracellular FFA levels in the studies of FFA metabolism. Therefore, we have assumed that $FFA_o = 7$ nM and $FFA_i = 3$ nM so that $\Delta C = 4$ nM. With these values, k_t predicted by eq 6, ranges from about 1.5 to 14 s^{-1} or is about 5−45-fold greater than the value of 0.3 s^{-1} for oleate flip-flop at 37 °C.

The characteristics of the lipid phase of the biological membrane may not be comparable with that represented by the bilayer of lipid vesicles. For example, the lipid composition of cell membranes is more complex than the EPC: cholesterol mixtures used in this study, the curvature of such membranes is also greater than for the >2000 Å GUV, and

the presence of proteins may modify the properties of the lipid phase. Moreover, given the uncertainties in estimating k_t, it is possible that the actual values might include the rate we observe in GUVs. At the very least, however, these results raise the possibility that flip-flop across the lipid phase of biological membranes might be too slow to accommodate the flux of FA needed to support metabolic activity.

REFERENCES

Anel, A., Richieri, G. V., & Kleinfeld, A. M. (1993) *Biochemistry 32*, 530−536.

Anversa, P., Giorgio, O., Massimo, M., & Loud, A. V. (1980) *J. Mol. Cell. Cardiol. 12*, 781−795.

Bassolino-Klimas, D., Alper, H. E., & Stouch, T. R. (1993) *Biochemistry 32*, 12624−12637.

Bevington, P. R., & Robinson, D. K. (1992) *Data reduction and error analysis for the physical sciences*, 2nd ed., McGraw-Hill, Inc., New York.

Bielefeld, D. R., Vary, T. C., & Neely, J. R. (1985) *J. Mol. Cell. Cardiol. 17*, 619−625.

Cardoza, J. D., Kleinfeld, A. M., Stallcup, K. C., & Mescher, M. F. (1984) *Biochemistry 23*, 4401−4409.

Comfurius, P. S., Smeets, E. F., Williamson, P., Schlegel, R. A., Bevers, E. M., & Zwaal, R. F. A. (1996) *Biochemistry 35*, 7631−7634.

Daniels, C., Noy, N., & Zakim, D. (1985) *Biochemistry 24*, 3286−3292.

Doody, M. C., Pownall, H. J., Kao, Y. J., & Smith, L. C. (1980) *Biochemistry 19*, 108−116.

Forsey, R. G. P., Reid, K., & Brosnan, J. T. (1987) *Can. J. Physiol. Pharmacol. 65*, 401−406.

Franzin, C. M., & Macdonald, P. M. (1997) *Biochemistry 36*, 2360−2370.

Glatz, J. F., Jacobs, A. E., & Veerkamp, J. H. (1984) *Biochim. Biophys. Acta 794*, 454−465.

Gomori, G. (1942) *J. Lab. Clin. Med. 27*, 955−960.

Gutknecht, J. (1988) *J. Membr. Biol. 106*, 83−93.

Homan, R., & Eisenberg, M. (1985) *Biochim. Biophys. Acta 812*, 485−492.

Hope, M. J., Bally, M. B., Webb, G., & Cullis, P. R. (1985) *Biochim. Biophys. Acta 812*, 55−65.

Kamp, F., Westerhoff, H. V., & Hamilton, J. A. (1993) *Biochemistry 32*, 11074−11086.

Kamp, F., Zakim, D., Zhang, F., Noy, N., & Hamilton, J. A. (1995) *Biochemistry 34*, 11928−11937.

Kleinfeld, A. M. (1995) in *Stability and permeability of lipid bilayers* (Disalvo, E. A., & Simon, S., Eds.) pp 241−258, CRC Press, Boca Raton.

Kleinfeld, A. M., & Chu, P. (1993) *Biophys. J. 64*, A306.

Kleinfeld, A. M., & Storch, J. (1993) *Biochemistry 32*, 2053−2061.

Kleinfeld, A. M., Chu, P., & Romero, C. (1997a) *Biophys. J. 72*, A406.

Kleinfeld, A. M., Chu, P., & Storch, J. (1997b) *Biochemistry 36*, 5702−5711.

Letizia, J. Y., & Phillips, M. C. (1991) *Biochemistry 30*, 866−873.

Linssen, M. C. J. G., Vork, M. M., de Jong, Y. F., Glatz, J. F. C., & van der Vusse, G. J. (1990) *Mol. Cell Biochem. 98*, 19−25.

Lopaschuk, G. D., Spafford, M. A., Davies, N. J., & Wall, S. R. (1990) *Circ. Res. 66*, 546−553.

Marassi, F. M., Shivers, R. R., & Macdonald, P. M. (1993) *Biochemistry 32*, 9936−9943.

Mason, J. T., & Huang, C. (1978) *Ann. NY Acad. Sci. 308*, 29−49.

Massey, J. B., Bick, D. H., & Pownall, H. J. (1997) *Biophys. J. 72*, 1732−1743.

McIntyre, J. C., & Sleight, R. G. (1991) *Biochemistry 30*, 11819−11827.

Meyuhas, D., & Lichtenberg, D. (1996) *Biophys. J. 71*, 2613−2622.

Morris, S. J., Bradley, D., & Blumenthal, R. (1985) *Biochim. Biophys. Acta 818*, 365−372.

Noy, N., Kelleher, D. J., & Scotto, A. W. (1995) *J. Lipid Res. 36*, 375−382.

Nozaki, Y., Lasic, D. D., Tanford, C., & Reynolds, J. A. (1982) *Science 217*, 366−367.

Richieri, G. V., & Kleinfeld, A. M. (1995a) *Anal. Biochem. 229*, 256−263.

Richieri, G. V., & Kleinfeld, A. M. (1995b) *J. Lipid Res. 36*, 229−240.

Richieri, G. V., Ogata, R. T., & Kleinfeld, A. M. (1992) *J. Biol. Chem. 267*, 23495−23501.

Richieri, G. V., Ogata, R. T., & Kleinfeld, A. M. (1994) *J. Biol. Chem. 269*, 23918−23930.

Richieri, G. V., Ogata, R. T., & Kleinfeld, A. M. (1995) *J. Biol. Chem. 270*, 15076−15084.

Richieri, G. V., Ogata, R. T., & Kleinfeld, A. M. (1996a) *J. Biol. Chem. 271*, 11291−11300.

Richieri, G. V., Ogata, R. T., & Kleinfeld, A. M. (1996b) *J. Biol. Chem. 271*, 31068−31075.

Richieri, G. V., Ogata, R. T., & Kleinfeld, A. M. (1997) *Mol. Cell Biochem.* (in press).

Srivastava, A., Singh, S., & Krishnamoorthy, G. (1995) *J. Phys. Chem. 99*, 11302−11305.

Stein, W. D. (1986) *Transport and diffusion across cell membranes*, Academic Press, Inc., Orlando.

Storch, J., & Kleinfeld, A. M. (1986) *Biochemistry 25*, 1717−1726.

Vork, M. M., Glatz, J. F. C., & Van der Vusse, G. J. (1993) *J. Theor. Biol. 160*, 207−222.

Walter, A., & Gutknecht, J. (1984) *J. Membr. Biol. 77*, 255−264.

Zhang, F., Kamp, F., & Hamilton, J. A. (1996) *Biochemistry 35*, 16055−16060.

Zucker, S. D., Goessling, W., Zeidel, M. L., & Gollan, J. L. (1994) *J. Biol. Chem. 269*, 19262−19270.

BI971440E